

Fortgeschrittenes physikalisches Praktikum

Wintersemester 2021/2022

Experiment

dopplerfree saturated spectroscopy on Rubidium

Group: 6

Date: 20.09.2021

Supervisor: Sanchayeeta Jana

Anna-Maria Pleyer · Dominik Müller



**UNIVERSITÄT
BAYREUTH**

Contents

1	Introduction	5
2	Fragen zur Vorbereitung	6
2.1	Kernspins und Quantenzahlen	6
2.2	Begriffe	6
2.3	Cross-Over Resonanzen	7
2.4	Strahlenteiler und $\frac{\lambda}{2}$ Plättchen	8
2.5	Hyperfeinstrukturkonstante und -übergänge	8
3	Protocol	11
4	Data Analysis	13
4.1	Detrending absorption spectrum and identification of lines	13
4.1.1	Cleaning the data	13
4.1.2	identification of the lines and transmission	16
4.2	Calculation of the energy level distance	19
4.2.1	Current-Wavelength Relation	19
4.2.2	Fabry-Perot-interferometer	19
4.2.3	Comparison of the two methods	21
4.3	Isotopes of Rubidium	22
4.4	Doppler free signal	24
4.4.1	Doppler free signal of the absorptiondips	24
4.4.2	Fitting of the Lorentz-profile	25
4.5	Hyperfineconstant	29
4.6	Temperature of the probe	30
5	Summary	31
A	Protocol	32
Bibliography		37

1 Introduction

Hyperfine structures are defined by small shifts in degenerate energy levels, so basically it's the smallest energy distance in atoms, molecules, or ions. The hyperfine structure arises from the energy of the nuclear magnetic dipole moment interacting with the magnetic field and the nuclear electric quadrupole moment in the electric field, at least in atoms.

One Possibility to measure such small distances as the hyperfine structures is the Doppler free spectroscopy which we will use in our experiment. During our experiment we will investigate rubidium and its hyperfine structure in more detail.

Rubidium is the chemical element with the symbol Rb and atomic number 37, so it's a alkali metal. Natural rubidium comprises two isotopes: ^{85}Rb (72%, stable), and 28% is slightly radioactive ^{87}Rb . Furthermore, rubidium can be handled as one electron system, which is useful for the following data analysis. However, in this experiment we will have a closer look at the fine and hyperfine structure of ^{87}Rb and ^{85}Rb , as well as the transition energy and the ratio its isotopes.

2 Fragen zur Vorbereitung

2.1 Kernspins und Quantenzahlen

Warum sind die Kernspins der beiden Rubidiumisotope unterschiedlich? Welche Quantenzahlen existieren im Grundzustand und den ersten beiden angeregten Zuständen für die beiden Rubidiumisotope und welche F-Quantenzahlen resultieren daraus?

Der Kernspins des ^{85}Rb beträgt $I_{85} = 5/2$. Der Kernspins des ^{87}Rb beträgt $I_{87} = 3/2$. Diese unterscheiden sich da man Isotope von Rubidium hat. Das ^{87}Rb -Atom hat 2 Neutronen mehr. Der Kernspin I ist die Summe der Summe von Spin und Bahndrehimpuls aller Nukleonen.

Für die verschiedenen Quantenzahlen folgt:

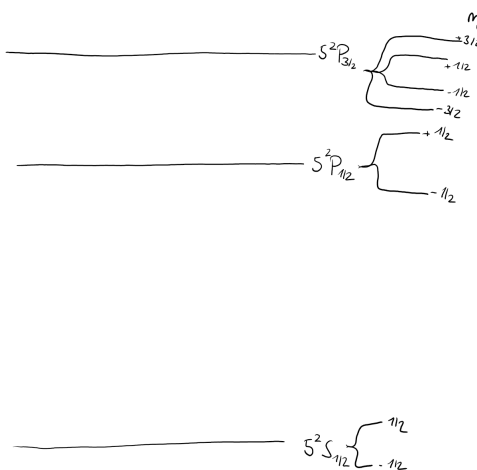


Figure 2.1: Quantenzahlen von Rubidium

Die F-Quantenzahlen kann man wie folgt bestimmen:

$$F = |J - I|, |J - I| + 1, \dots, J + I - 1, J + I \quad (2.1)$$

Somit hat ^{85}Rb eine F Quantenzahl von 2 bis 3 und ^{87}Rb eine F Quantenzahl von 1 bis 2 für den $S/P_{1/2}$. Für den Zustand $P_{3/2}$ hat ^{85}Rb eine F Quantenzahl von 1 bis 4 und ^{87}Rb eine F Quantenzahl von 0 bis 3.

2.2 Begriffe

Informieren Sie sich zu den Begriffen 'natürliche Linienbreite', 'Doppel-Verbreiterung', 'homogene/inhomogen Verbreiterung' und 'Sättigungsverbreiterung'.

Natürliche Linienbreite und homogene/inhomogene Verbreiterung

Die **natürliche Linienbreite** basiert auf der Energie-Zeit-Unschärferelation. Die Bestimmung der Lebensdauer und der exakten Energie eines angeregten Zustandes ist nicht möglich. Dies führt zu einer statischen Verbreiterung der Linienbreite.

Unter Verbreiterungsmechanismen versteht man die Vergrößerung der Linienbreite über die natürliche Linienbreite hinaus. Hierbei unterscheidet man zwischen zwei Arten:

Die **homogene Verbreiterung** tritt auf, wenn die Emissionswahrscheinlichkeit für eine bestimmte Frequenz für alle Teilchen gleich groß ist. Hierzu zählen z.B. Druckverbreiterung und Sättigungsverbreiterung.

Die **inhomogenen Verbreiterung** tritt auf, wenn die Emissionswahrscheinlichkeit für eine bestimmte Frequenz nicht für alle Teilchen gleich groß ist. Hierzu zählen z.B. Doppelverbreiterung.

Doppelverbreiterung

Dort hängt die Wahrscheinlichkeit von der Geschwindigkeit der Moleküle ab. Diese bewegen sich auf dem Detektor zu und wieder weg, was eine Änderung der Frequenz zur Folge hat (Doppler-Effekt). Da nun die Geschwindigkeiten nicht gleichmäßig verteilt sind (Stefan-Boltzmann-Verteilung), kommt es zu einer inhomogenen Linienverbreiterung.

Sättigungsverbreiterung

Eine weitere Linienverbreiterung ist die Sättigungsverbreiterung. Hier wächst die Linienbreite an, da der Übergangszustand durch eine Pumpe größtenteils gesättigt sind. Tritt dies ein, werden mehr Photonen am Rand der Linie absorbiert, was zu einer homogenen Verbreiterung der Spektrallinie führt.

2.3 Cross-Over Resonanzen

Was sind 'Cross-Over Resonanzen' und wie entstehen diese?

Liegen in einem Spektrum zwei Niveaus nahe nebeneinander, so gibt es eine Überkreuzung (*Cross-Over*). Dadurch entsteht eine Weitere Linie im Spektrum.

Erklärt werden kann dies dadurch, dass die entgegengesetzte Dopplerverschiebung des Pump- und Abfangstrahls gleich groß, aber entgegengesetzt ist. Dadurch tritt die Entvölkerung durch die Pumpe und Absorption durch den Abfangstrahl in den gleichen Geschwindigkeitsklassen auf, wodurch die Absorption verringert ist (vgl. Wikipedia, 2021a).

2.4 Strahlenteiler und $\frac{\lambda}{2}$ Plättchen

**Wofür werden im Versuch zwei Strahlenteilerwürfel benötigt, die polarisierend sind?
Wozu wird das $\frac{\lambda}{2}$ Plättchen und das Filterrad gebraucht?**

Mithilfe eines Strahlteilers kann man, wie es der Name bereits verrät, einen einzelnen Strahl in zwei Teilstrahlen aufteilen.

In der folgenden Abbildung 2.2 ist dies schematisch aufskizziert:

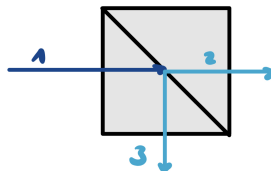


Figure 2.2: Schematische Skizze eines Strahlenteilerwürfels

Bei dem Spezialfall *polarisierenden Strahlenteilerwürfel* ist das Teilungsverhältnis abhängig vom Polarisationswinkel des einfallenden Lichts.

Alle Strahlanteile einer Polarisationsrichtung werden am Strahlteiler transmittiert, die restlichen Strahlanteile werden senkrecht zur Einfallsebene reflektiert.(vgl. Wikipedia, 2021c)

In unserem Versuch wird ein solcher Strahlteiler genutzt, um die Intensitäten des Pump- bzw. Probestrahls einzustellen zu können.

Das $\frac{\lambda}{2}$ Plättchen oder auch Verzögerungsplatte ist ein optisches Bauelement, welches die Polarisierung einer elektromagnetischen Welle ändern kann. Das heißt in unserem Versuch sorgt das $\frac{\lambda}{2}$ Plättchen zusammen mit einem linearen Polarisator dafür, dass der eintreffende Strahl linear polarisiert wird. Zusätzlich sorgt das Plättchen für einen Phasensprung um π . Dies hat zur Folge, dass die Polarisationsrichtung nach dem Auftreffen auf das Plättchen um 90° gedreht ist, im Vergleich zu vor dem Eintritt in das Plättchen.(vgl. Wikipedia, 2021d)

Mithilfe dem Filterrads lassen sich die Intensitäten einstellen und anpassen.

2.5 Hyperfeinstrukturkonstante und -übergänge

**Wie kann man aus den gewonnenen Daten die Hyperfeinstrukturkonstanten berechnen?
Welche Hyperfeinübergänge sind im Spektrum zu erwarten?**

Im Versuch werden die Absorptionsspektren der Rubidiumisotope gemessen. Mithilfe der gemessenen Absorptionslinien lassen sich Aussagen über die Absorptionsenergien für die Übergänge treffen. Die entsprechende Energie ist wie folgt definiert:

$$\Delta E_{HFS} = \frac{a}{2}[F(F+1) - J(J+1) - I(I+1)] \quad (2.2)$$

Wobei F für den Gesamtdrehimpuls, J für den Gesamtdrehimpuls der Hülle und I für den Kernspin steht.

Diese Komponenten sind bereits bekannt und so fehlt nur noch a.

a ist die sogenannte Hyperfeinstrukturkonstante und ist wie folgt definiert:

$$a = \frac{g_I \cdot \mu_k}{\sqrt{J(J+1)}} \quad (2.3)$$

2.5 Hyperfeinstrukturkonstante und -übergänge

Hierbei wird g_I als Landé-Faktor bezeichnet und μ_k steht für das Kernmagneton.

Das Kernmagneton wird wie folgt berechnet und m_p steht hierbei für die Protonenmasse:

$$\mu_k = \frac{e \cdot \hbar}{2m_p} = 5,05783 \cdot 10^{-27} \frac{J}{T}$$

(vgl. Köhler, 2021)

Die folgenden Graphen zeigen die erlaubten Hyperfeinübergänge der Isotope ^{85}Rb und ^{87}Rb für die beiden möglichen D-Linien (entnommen Steck, 2013, 2015).

Hierbei wurden die allgemein gültigen Auswahlregeln mitberücksichtigt und die möglichen Übergänge eingezzeichnet:

$$\Delta L = \pm 1$$

$$\Delta I = 0, \pm 1$$

$$\Delta J = 0, \pm 1$$

$$\Delta F = 0, \pm 1$$

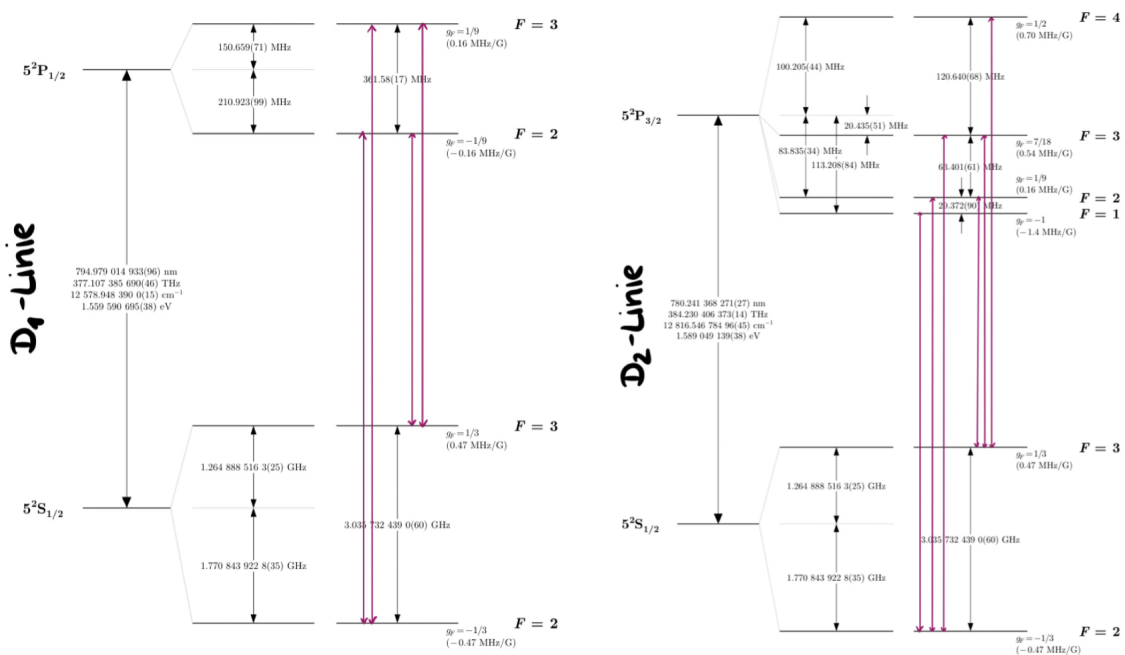


Figure 2.3: Übergänge der D1- bzw. D2-Linie von ^{85}Rb

2 Fragen zur Vorbereitung

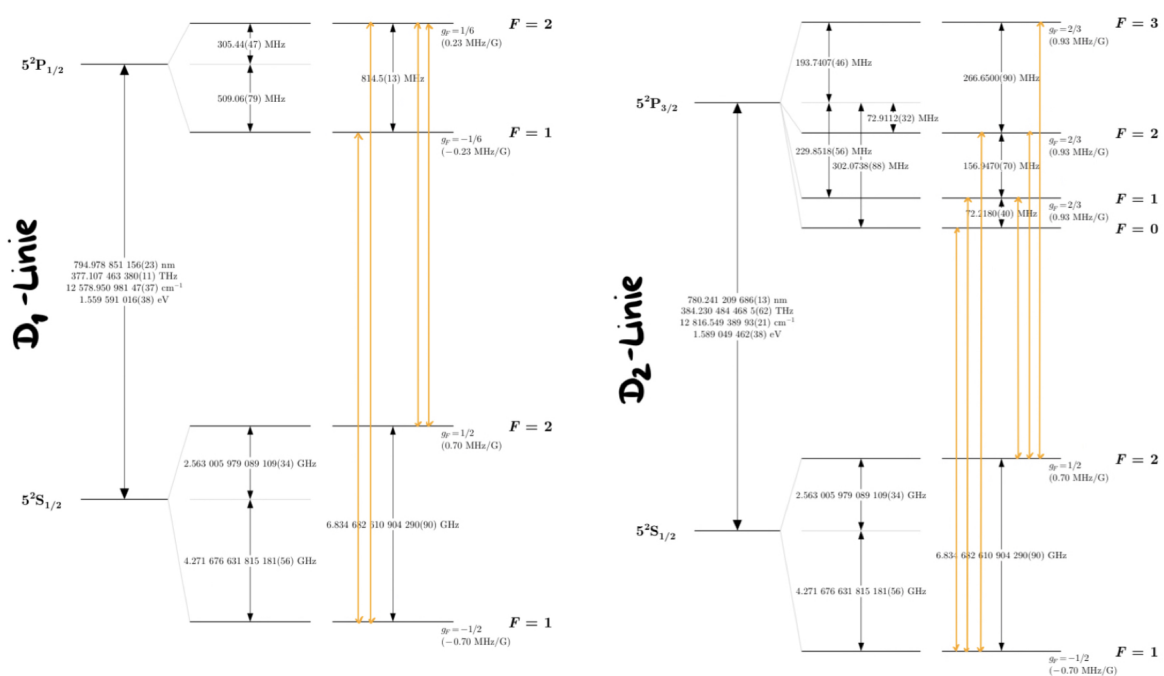


Figure 2.4: Übergänge der D1- bzw. D2-Linie von ⁸⁷Rb

3 Protocol

The following graph shows our experimental setup during the experiment. To make this clear, the corresponding optical components have been marked.

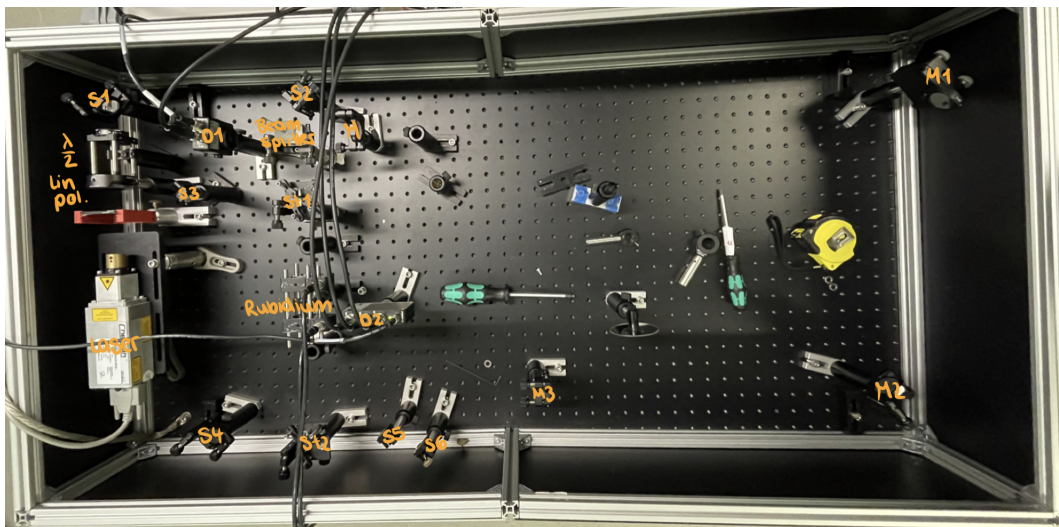


Figure 3.1: Picture of the experimental setup

As can be seen, the experimental setup was constructed according to the diagram shown in the manual 3.2.

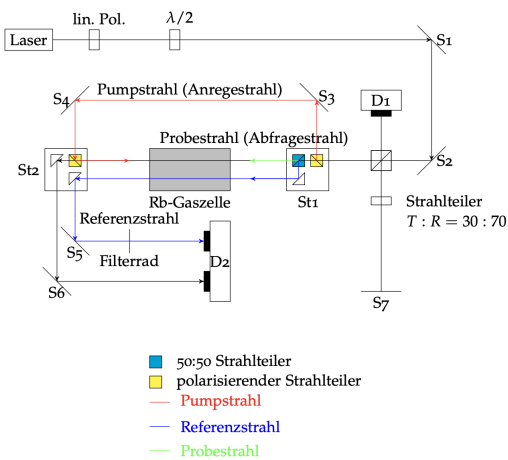


Figure 3.2: figure of the experimental setup from the instruction

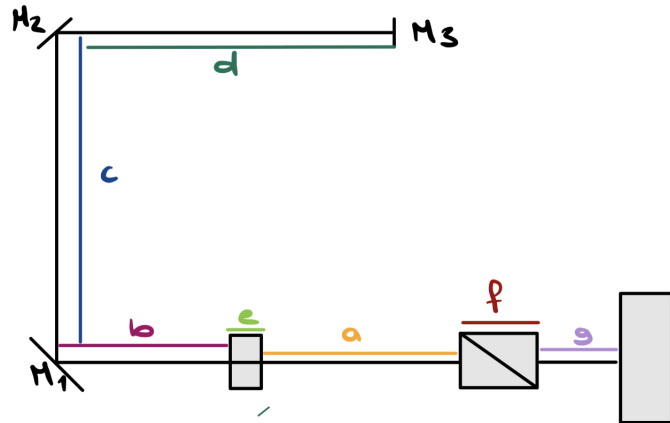
Before measurement startet we build the set up after the manual and then the different components i.e. the mirrors were aligned and adjusted according to the instructions.

3 Protocol

After everything was adjusted we got used to the measuring program.
The different channels are defined as follows:

- Channel 0 (Ai0): Diffrence
- Channel 1 (Ai1): Sample Beam
- Channel 2 (Ai2): /
- Channel 3 (Ai3): Reference Beam
- Channel 4 (Ai4): Fabry Perot Interferometer
- x-axis: laser current in mA
- y-axis: amplitude in V

During the experiment some distances were measured as well, those are illustrate in the following plot:



The corresponding values are the followings:

$$a = (7.9 \pm 0,3) \text{ cm} \quad (3.1)$$

$$b = (72.0 \pm 0,3) \text{ cm} \quad (3.2)$$

$$c = (35.0 \pm 0,3) \text{ cm} \quad (3.3)$$

$$d = (42.0 \pm 0,3) \text{ cm} \quad (3.4)$$

$$e = (0.7 \pm 0,1) \text{ cm} \quad (3.5)$$

$$f = (2.5 \pm 0,1) \text{ cm} \quad (3.6)$$

$$g = (7.4 \pm 0,1) \text{ cm} \quad (3.7)$$

$$(3.8)$$

The used measuring instruments are to be found in the measurement protocol in appendix A.

4 Data Analysis

4.1 Detrending absorption spectrum and identification of lines

The given task should only be done for one temperature. The chosen temperature is 60°C in our measurement because here the lines are clear in comparison with the other temperatures. Also, the peaks at the temperature 60°C are the best defined ones. 60°C was the desired temperature, however we only could get a temperature of $(56.0 \pm 0.2)^\circ\text{C}$.

4.1.1 Cleaning the data

First of all, the mess data should be considered. Therefore, have a closer look at the following plot:

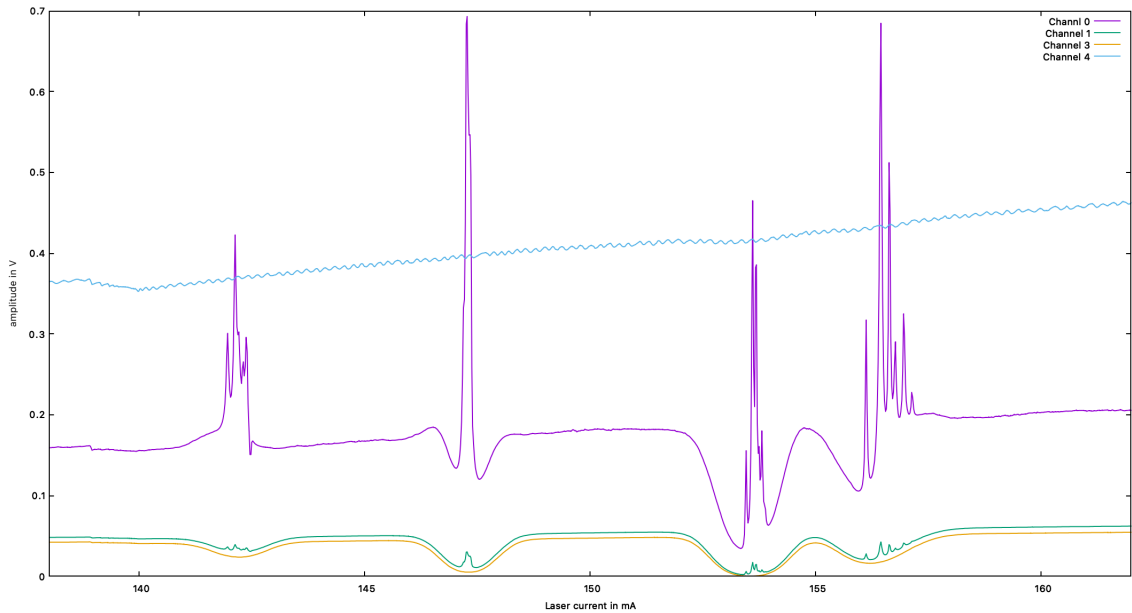


Figure 4.1: unadjusted mess data

In this plot channel 0 is the Difference, channel 1 is the absorption spectrum, channel 3 is the reference measurement and channel 4 is the Fabry Perot Interferometer.

As can be seen from the plot, the measured values appear to be subject to a slight slope. This increasing trend seems to distort them. So, it's obvious that the measured data need to be adjusted and freed from this trend. In order to be able to implement this, one must first fit a straight line at the increasing trend. Afterwards this straight line will be subtracted from the mess data and we receive the trend-free and adjusted data.

4 Data Analysis

Unfortunately, the slope of the increasing trend is only in the channel 0, channel 1 and channel 3 similar. Accordingly, you have to calculate a second fit-line and apply it only to channel 4.

First fitting line:

For the first fitting line (for the channel 1, channel 2 and channel 3) we use only one channel to do the fitting line. We can apply this fitting-line to the other mess data as well, since as already mentioned above, the slope of the three channels is similar.

After the fit has just been determined, the program GNUMplot is used for this purpose, we subtract the line from the mess data.

The following plot is intended to illustrate as an example how the just described progress proceed:

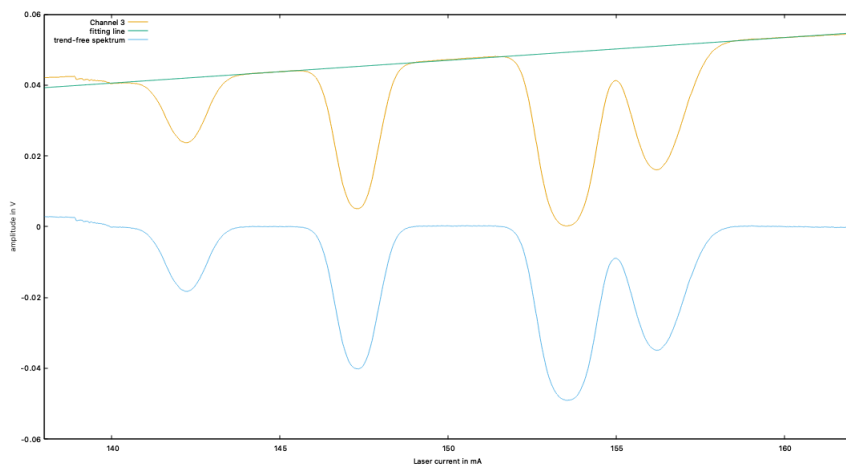


Figure 4.2: unadjusted data (orange), fitting line (green) and trend-free data (blue).

This is done for the rest of the data as well, but not shown explicitly again.

Second fitting line:

For the fitting line for channel 4 we use as well GNUMplot. After we found the correct fitting line, we subtract this line as well from the original mess data to get the adjusted mess data.

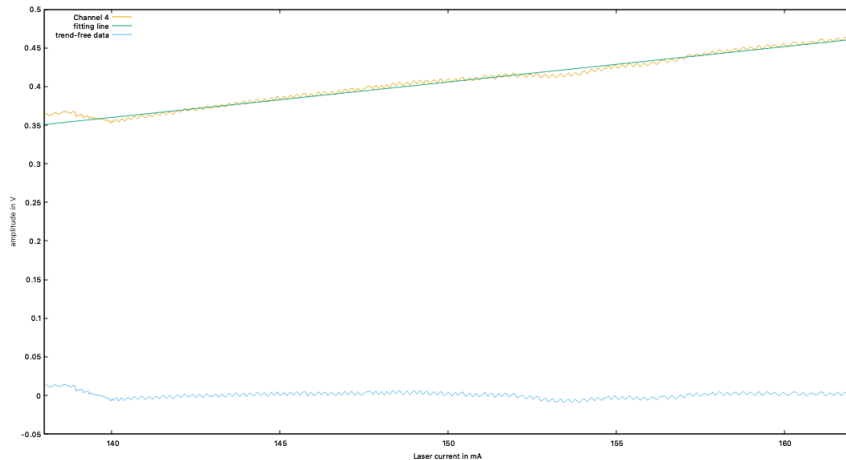


Figure 4.3: unadjusted mess data (orange), fitting line (green) and adjusted mess data (blue) of channel 4

4.1 Detrending absorption spectrum and identification of lines

The following plot shows, why it was necessary to do a second fitting line:

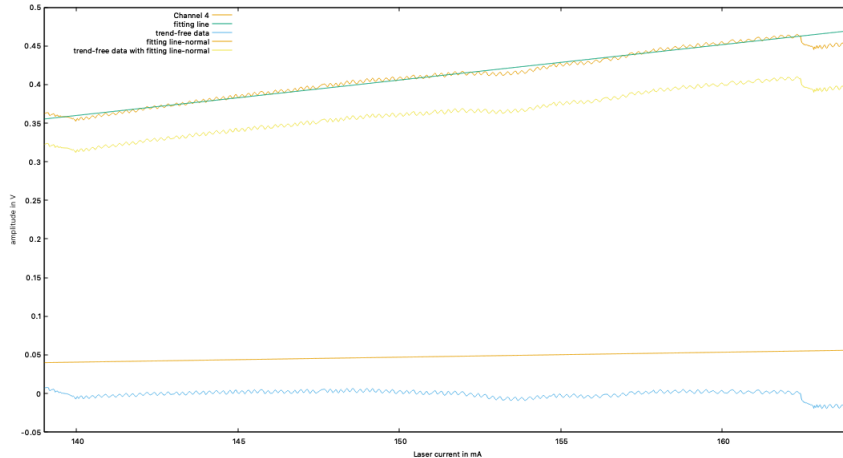


Figure 4.4: first fitting line (orange) and second fitting line (green) of channel 4 in comparison

As you can see from this plot, it was necessary to calculate a new fitting line. The fitting line (orange) for the channels 0, 1 and 3 has a too low fitting line gradient to really clean up the FPI data. So a second line (green) was calculated and we receive the adjusted mess data (blue) of channel 4.
At the end the whole adjusted mess data for all channels look like:

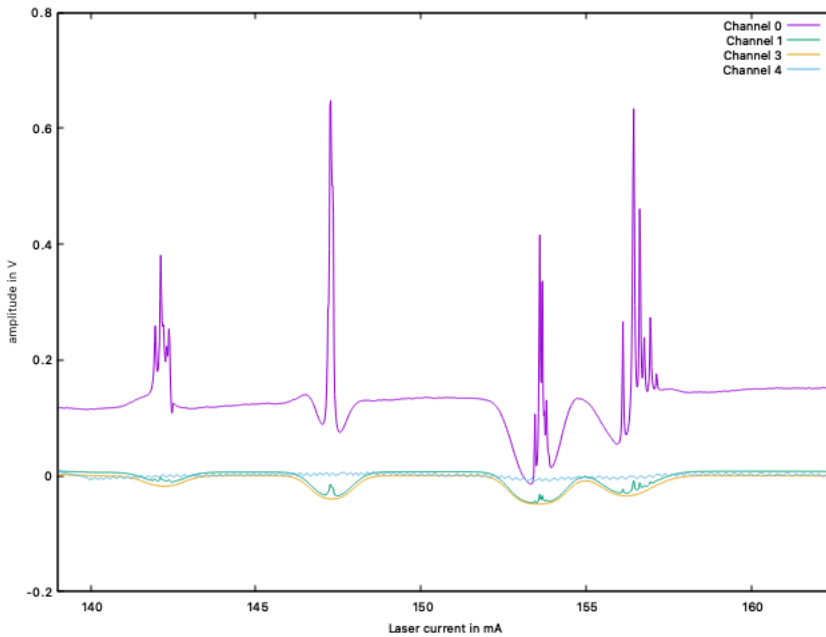


Figure 4.5: adjusted mess data for all channels

4 Data Analysis

4.1.2 identification of the lines and transmission

In the next sub-task, the lines in the absorption spectrum should be named. First of all, we limit the scan range again, instead of using the full scan range we will only be using the area from 140 mA to 160 mA. We determined that area because there is no visible mode jump in between.

To define the peaks in the spectrum we fit a Gauss curve over the four lines, for this we are using Python.

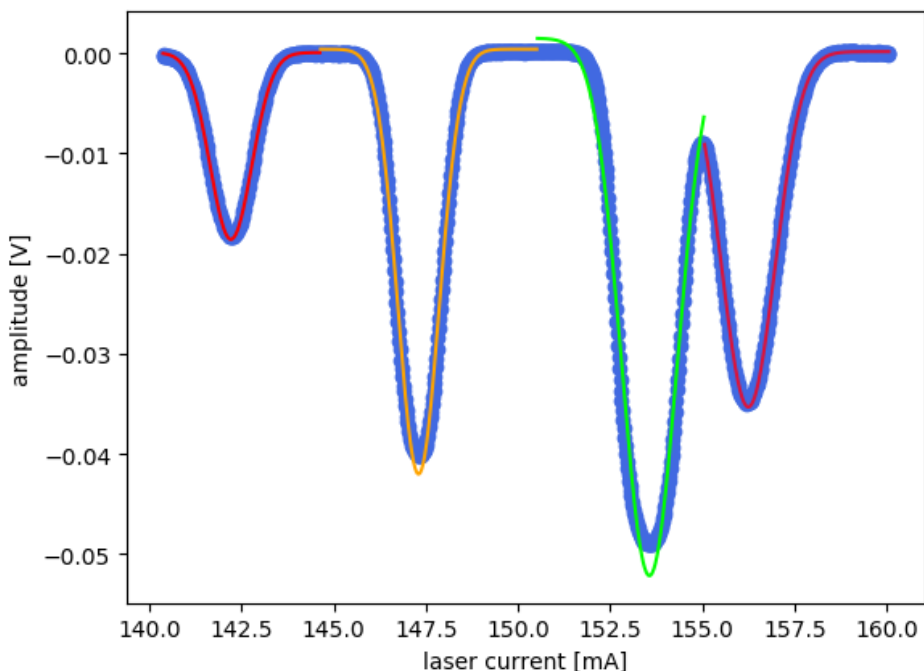


Figure 4.6: Gaussian fitting curve for the different peaks

Using a python script you get the exact position of the dips (I in mA) in the spectrum. With the help of the Laser current - wavelength relation it is possible to convert the current into wavelength.

4.1 Detrending absorption spectrum and identification of lines

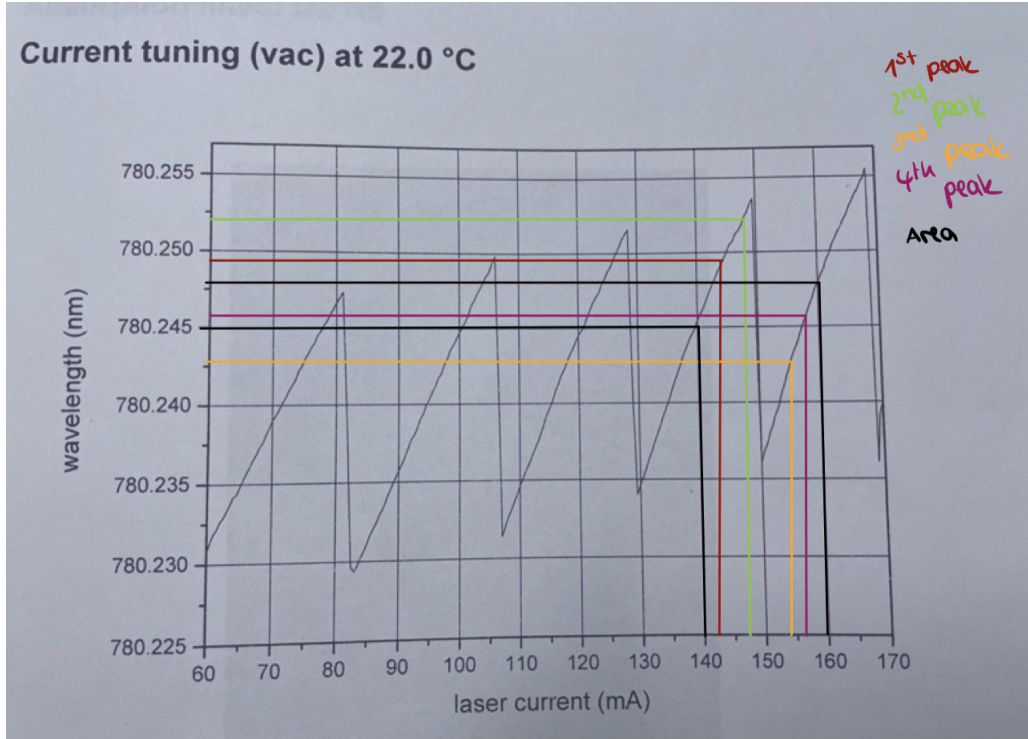


Figure 4.7: conversion between laser current and wavelength of the laser

As you can see from the figure 4.7 it's challenging to find out the exact wavelengths from the photographed current-wavelength relation. The extracted values are inaccurate and have a big error. Therefore, a read-off error of $s_\lambda = 0.0005\text{nm}$ is set. Nevertheless, we determined as best as possible the wavelength and afterwards we calculated it into the frequency with the following equation:

$$\nu = \frac{c}{\lambda} = \frac{299792458 \frac{\text{m}}{\text{s}}}{\lambda} \quad (4.1)$$

Here stands c for the speed of Light.

The error propagation for the frequency:

$$s_\nu = \frac{c}{\lambda^2} \cdot s_\lambda = 0.0000025 \cdot 10^{14} \text{ Hz} \quad (4.2)$$

The results are shown in the following table:

Peak	I in mA	λ in nm	ν in 10^{14} Hz
1	142.2	780.2490 ± 0.0005	3.8422665 ± 0.0000025
2	147.3	780.2522 ± 0.0005	3.8422507 ± 0.0000025
3	153.6	780.2426 ± 0.0005	3.8422979 ± 0.0000025
4	156.2	780.2462 ± 0.0005	3.8422803 ± 0.0000025

Table 4.1: Laser current, wavelength and frequency of the four peaks

Now that we have determined the wavelengths and frequencies of our lines, we have to compare them with appropriate literature values (see Steck, 2013, 2015).

4 Data Analysis

Since in the table 4.1 only a wavelength of approx. 780 nm appears, which is not surprising considering which laser we used during the experiment, the literature values are only those of a D2-line.

Isotopes	F	ν_{lit} in 10^{14} Hz
^{87}Rb	2	3.842279
^{85}Rb	3	3.842291
^{85}Rb	2	3.842321
^{87}Rb	1	3.842348

Table 4.2: Literature value for the frequency of transitions

The next step is to compare the literature values with ours and then we should be able to determine the lines.

But unfortunately, even if we consider our values and their error bars with the literature values they don't match.

One possible reason for this might be that the given laser-current characteristic is not so accurate for current configuration. We used an area between two mode jumps, so it's naturally to think that there is an increasing of the wavelength along to first to fourth peak. So, as we just discussed the wavelength should be increasing, so the frequency should be decreasing. However, if you expand the error range and keep the recently discussed arguments in mind, we can identify the lines:

Peak	Isotopes	F	ν in 10^{14} Hz
1	^{87}Rb	1	3.8422979
2	^{85}Rb	2	3.8422803
3	^{85}Rb	3	3.8422665
4	^{87}Rb	2	3.8422507

Table 4.3: identification of the Lines

4.2 Calculation of the energy level distance

In the following task we should calculate the energy level distance of the absorption spectrum with two different methods. We limit the scan range again, instead of using the full scan range we will only be using the area from 140 mA to 160 mA. We determined that area because there is no visible mode jump in between.

4.2.1 Current-Wavelength Relation

As already done above, for this method we also use the current-wavelength relation figure 4.7.

After the wavelength and the current have been determined (Table: 4.1), the energy level can be calculated for the four dips:

$$E_i = h \cdot \nu = \frac{hc}{\lambda_i} \quad (4.3)$$

In this formula c stands again for the speed of light and h stands for the Planck-constant.

The error of the energy is calculated as the following:

$$s_{E_i} = \frac{hc}{\lambda_i^2} \cdot s_\lambda \quad (4.4)$$

Here is the error of λ the same as in the task before: $s_\lambda = 0.0005$ nm.

Next step is to calculate the energy level distance, therefore, we use the following equation:

$$\Delta E = |E_i - E_{i+1}| \quad (4.5)$$

With the formula mentioned above, the following values are obtained:

Peak	I in mA	λ in nm	E in 10^{-24} J	ΔE in 10^{-24} J
1	142.2	780.2490 ± 0.0005	254591.3 ± 0.2	1.04 ± 0.23
2	147.3	780.2522 ± 0.0005	254590.2 ± 0.2	3.13 ± 0.23
3	153.6	780.2426 ± 0.0005	254593.4 ± 0.2	1.17 ± 0.23
4	156.2	780.2462 ± 0.0005	254592.2 ± 0.2	

Table 4.4: Laser current, wavelength and frequency of the four peaks

4.2.2 Fabry-Perot-interferometer

In this task we want to determine the energy level distance with a second method. This time we will use the Fabry-Perot-Interferometer (FPI).

Firstly, we need to calculate the free spectral range of the used FPI.

$$\Delta\nu_{FSR} = \frac{c}{2 \cdot n \cdot d} = \frac{c}{2 \cdot d} = 1.154200963 \cdot 10^8 \text{ Hz} \quad (4.6)$$

In the second equal sign was used that we have a refractive index of $n = 1$ because the medium is air. c is again the speed of light and d is the measured distance of the FPI, in our case its $d = c + d = 0.77$ m. Now we need to calculate the error of $\Delta\nu_{FSR}$, for this we use the error propagation:

$$s_{\Delta\nu_{FSR}} = \frac{\partial \Delta\nu_{FSR}}{\partial d} \cdot s_d = \frac{c}{2 \cdot d^2} \cdot s_d = 758456.21 \text{ Hz} \quad (4.7)$$

4 Data Analysis

In the formula above the error of d is a read-off error again and its value is: $s_d = 0.003 \text{ m}$. With the preceding values follows for the free spectral range:

$$\Delta\nu_{FSR} = (11.54 \pm 0.08) \cdot 10^7 \text{ Hz} \quad (4.8)$$

In order to get the distances of the energy levels in the absorption spectrum you first have to count the number of dips m from the figure:

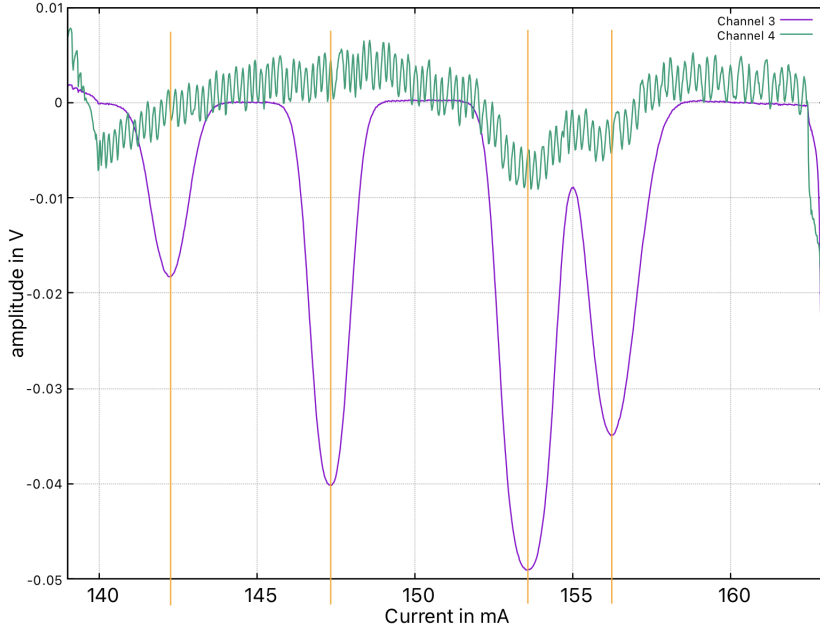


Figure 4.8: trend free data with the drawn lines for the certain region.

However, only the dips in a certain region, i. e. between two different peaks, need to be considered.

Finally we get the energy level distance using the following equation:

$$\Delta E = m \cdot h \cdot \Delta\nu_{FSR} \quad (4.9)$$

Here is m the number of the counted peaks in the specific area and h is again the Planck-constant. Finally, we need to have a closer look at the error propagation of ΔE .

$$s_{\Delta E} = \sqrt{\left(\frac{\partial \Delta E}{\partial m} \cdot s_m\right)^2 + \left(\frac{\partial \Delta E}{\partial \Delta\nu_{FSR}} \cdot s_{\Delta\nu_{FSR}}\right)^2} = h \sqrt{(\Delta\nu_{FSR} \cdot s_m)^2 + (m \cdot s_{\Delta\nu_{FSR}})^2} \quad (4.10)$$

The error of m is again a read-off error, because you have to read out the corresponding dips from a photo. As mentioned before it is not really accurate to read out of an photograph.

Distance	m	$\Delta E \text{ in } 10^{-24} \text{ J}$
1-2	24 ± 1	1.828 ± 0.077
2-3	29 ± 1	2.209 ± 0.077
3-4	12 ± 2	0.914 ± 0.152

Table 4.5: Distance of the energy level between two dips

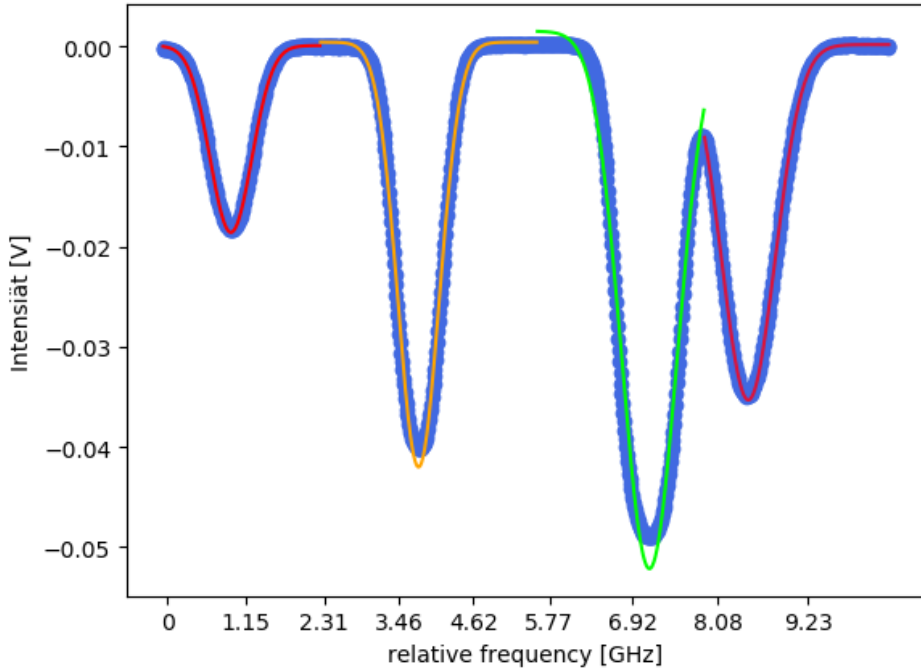


Figure 4.9: Full plot of the data with relative frequency as x-axis

4.2.3 Comparison of the two methods

As you can see in the two tables 4.4 and 4.5 both methods lead to similar values if you only compare the order of magnitude.

Both methods are not really accurate. In both cases, the corresponding values had to be determined by means of pictures. However, the first method was even more inaccurate because one had to read out the wavelength with a second image. This significantly increases the uncertainty of this method. In the case of the second method, however, you also had to read the dips out of a graph and the area by which you have to count them. But due to the “zoomed in” area the difficulty is not too great to see the dips. Nevertheless, this method is probably a bit more accurate because measured values such as the distance of the FPI were also used here.

4.3 Isotopes of Rubidium

To calculate the ratio of the Rubidium isotopes, four gaussian curves are fitted into the absorption spectrum. The gaussian curve is defined as:

$$f(x) = -a \cdot \exp\left(\frac{-(x-b)^2}{2c^2}\right) + d \quad (4.11)$$

Where a is the amplitude, b the peak-position, c the width and d the distance from the y-axis. From the fitting you yield:

Dip	$a (10^{-2})$	b	c	d
1 (^{85}Rb)	5,34	153,57	0,747	1,136
2 (^{87}Rb)	3,56	156,25	0,726	2,839
3 (^{87}Rb)	2,10	163,08	0,253	2,799
4 (^{85}Rb)	5,01	167,46	5,019	3,204

Table 4.6: Fitting parameter of the gaussian-curves

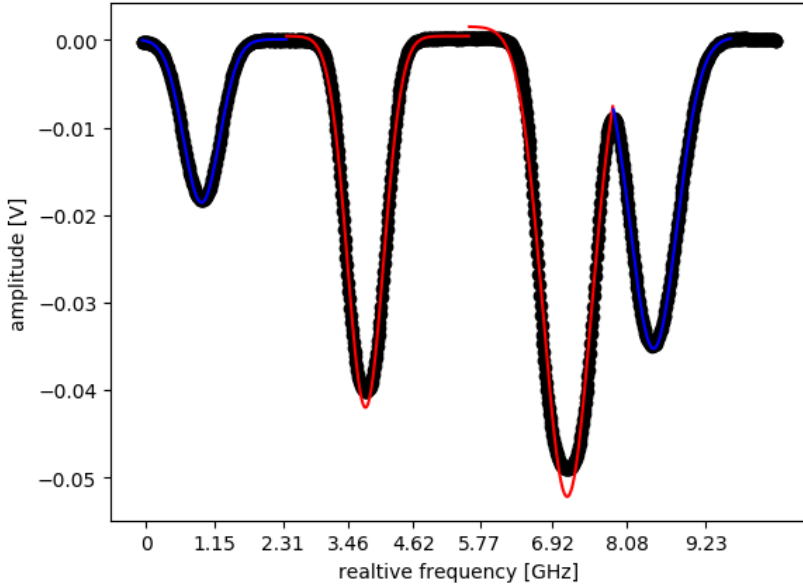


Figure 4.10: Fit of the Gauss-curves; Red: (^{85}Rb), Blue: (^{87}Rb)

Now we calculate the integral over the gaussian curves:

$$\int_{-\infty}^{\infty} -a \cdot \exp\left(\frac{-(x-b)^2}{2c^2}\right) dx = a\sqrt{2\pi c^2} \quad (4.12)$$

It follows:

Dip	Area
1 (^{87}Rb)	0,013302
2 (^{85}Rb)	0,063096
3 (^{85}Rb)	0,099945
4 (^{87}Rb)	0,064184

Table 4.7: Areas of the dips

Now the individually Areas of the corresponding isotopes are summed up and divides through the whole area:

Isotope	measured	theoretical
(^{85}Rb)	0,6778	0,7217
(^{87}Rb)	0,3222	0,2783

Table 4.8: Distribution of the isotopes

The calculated values are close to the theoretical ones. The difference is about 5%.

4.4 Doppler free signal

4.4.1 Doppler free signal of the absorptiondips

Here are the Doppler-free signals of the absorption dips. We used here the balanced channel:

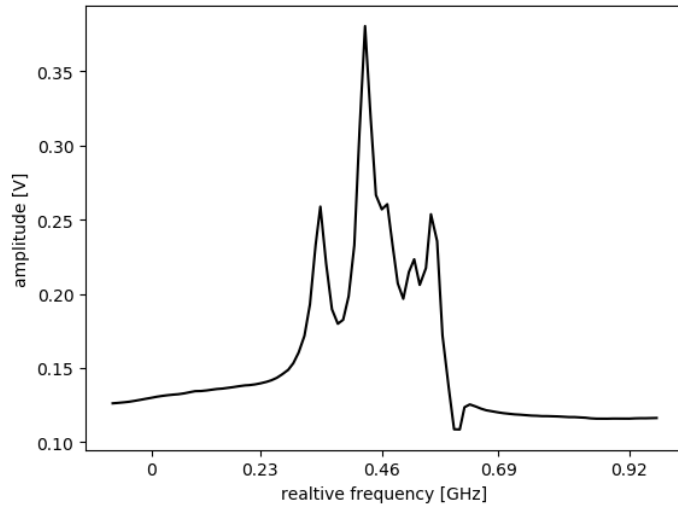


Figure 4.11: First dip in the whole spectrum

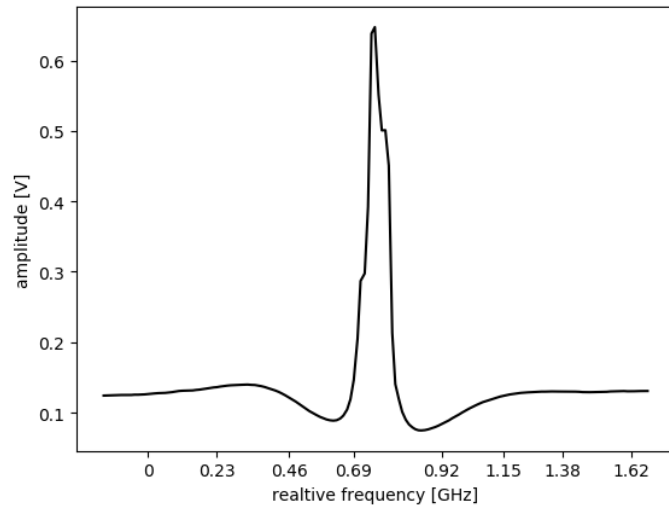


Figure 4.12: Second dip in the whole spectrum

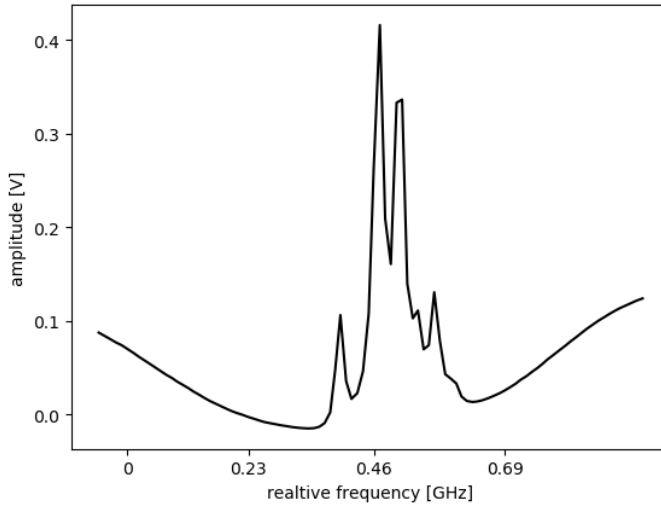


Figure 4.13: Third dip in the whole spectrum

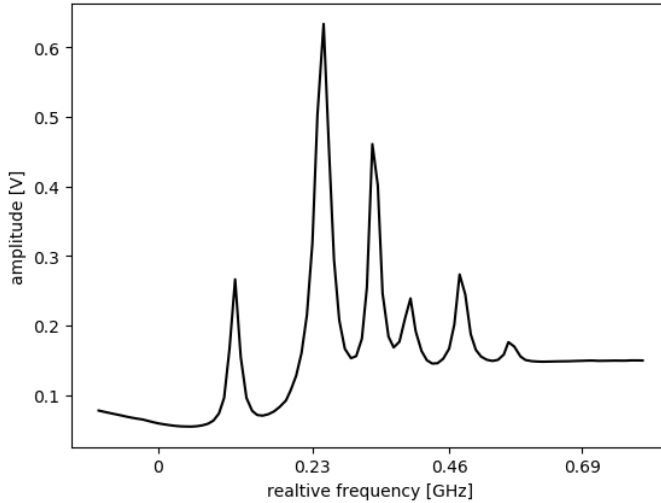


Figure 4.14: Fourth dip in the whole spectrum

4.4.2 Fitting of the Lorentz-profile

At first we select one measurement of one peak (in our case peak number one) of the spectrum. Then we separate the data of the peak to each dip and fit a lorentz-profile to it. The lorentz-profile is defined as (Wikipedia, 2021b):

$$f(x) = \frac{a \cdot b}{(x - b)^2 + c^2} + d \quad (4.13)$$

Where a is the amplitude, b the maximum, c the width of the peak and d the shift on the y-axis. Then we fit the lorentz-profile to each dip of one peak.

4 Data Analysis

After it the result looks like this:

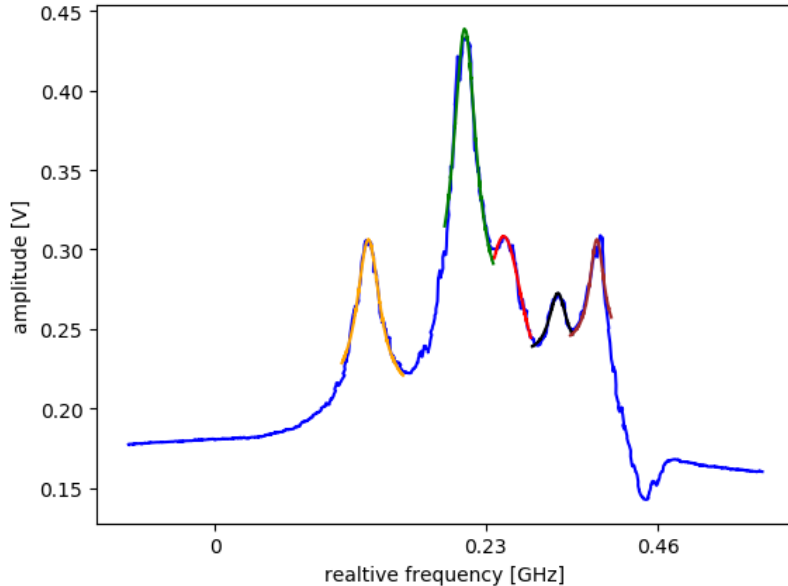


Figure 4.15: Peak No.1 with the lorentz-fit

Here is a table with the resulting variables:

Dip	a	b	c	d
1	0,31	141,88	0,45	0,18
2	0,42	142,05	0,09	0,30
3	0,31	142,13	0,05	0,24
4	0,27	142,23	0,11	0,25
5	0,31	142,30	0,21	0,14

Table 4.9: Fitting parameters of the lorentz fit

In the plot are smaller and larger dips. Ther larger dips are likely coming from 'Cross-over signals'.

To determine the energetic distance between the tops of two dips, we use the conversion of the current into wavelength:

$$\Delta E_{i,i+1} = \frac{hc}{\lambda_{i+1}} - \frac{hc}{\lambda_i} = hc \left(\frac{1}{\lambda_{i+1}} - \frac{1}{\lambda_i} \right) \quad (4.14)$$

To convert current into wavelength we fit a line to the current-wavelength correspontentive and get:

$$\text{wavelength} = 1,3 \cdot 10^{-3} \cdot \text{current} + 780,063 \quad (4.15)$$

So we get:

Dip (i)	λ (nm)
1	$780,247444 \pm 0,000013$
2	$780,247665 \pm 0,000013$
3	$780,247769 \pm 0,000013$
4	$780,247899 \pm 0,000013$
5	$780,247990 \pm 0,000013$

Table 4.10: Wavelength of the dips

And for the distance

Dip ($i \rightarrow i+1$)	$\Delta E_{i,i+1} (10^{-26} \text{ J})$	$\Delta \nu_{i,i+1}$ (MHz)
1to2	$7,2111 \pm 0,59989$	$108,8298 \pm 9,0534$
2to3	$3,3935 \pm 0,59989$	$51,21404 \pm 9,0532$
3to4	$4,2418 \pm 0,59989$	$64,01753 \pm 9,0534$
4to5	$2,9693 \pm 0,59989$	$44,81225 \pm 9,0534$

Table 4.11: Energetic distances of the dips

If you look now into the datasheet of the 85-Rb line (Steck, 2013), you can see that two transitions are 'perfectly' measured. The transition 2→3 and 4→5 are most likely Cross-over signals.

If you now compare both lines you get:

F-transition	$\Delta \nu_{meas.}$ (MHz)	$\Delta \nu_{theo.}$ (MHz)
4→3	$108,8298 \pm 9,0534$	$120,640$
3→2	$64,01753 \pm 9,0534$	$63,401$

Table 4.12: Comparism of experiment and theory

You can see our measured values are similar to the theoretical values (Steck, 2013).

If we use the FPI to calculate the frequency distances, first we measure the mean width of one period of the FPI:

$$\Delta T = (0,21 \pm 0,01) \text{ mA} \quad (4.16)$$

For this we used the full measurement of all lines, because it has the most FPI-Peaks in it and the peaks themself are relative sharp and not noisy.

So the frequency distance per 'mA' is:

$$\Delta f = \frac{\Delta x}{\Delta T} \cdot \Delta \nu_{FSR} \quad (4.17)$$

$$\Delta f = 549,52 \frac{\text{MHz}}{\text{mA}} \cdot \Delta x \quad (4.18)$$

Here is Δx the distance between two dips of the peak.

For the error follows:

$$s_{\Delta f} = \sqrt{\left(\frac{\partial \Delta f}{\partial \Delta x} \cdot s_{\Delta x}\right)^2 + \left(\frac{\partial \Delta f}{\partial \Delta T} \cdot s_{\Delta T}\right)^2 + \left(\frac{\partial \Delta f}{\partial \Delta \nu_{FSR}} \cdot s_{\Delta \nu_{FSR}}\right)^2} \quad (4.19)$$

$$s_{\Delta f} = \sqrt{\left(\frac{s_{\Delta x}}{\Delta f} \cdot \Delta \nu_{FSR}\right)^2 + \left(\frac{\Delta x}{\Delta T^2} \cdot s_{\Delta T} \cdot \Delta \nu_{FSR}\right)^2 + \left(\frac{\Delta x}{\Delta f} \cdot s_{\Delta \nu_{FSR}}\right)^2} \quad (4.20)$$

4 Data Analysis

We do it this way, because the distance between two peaks is less than one full period of the FPI. With the fitted parameters (the position of the dips of the peaks) we can now calculate the frequency distances of the dips:

Dip (i→i+1)	$\Delta\nu_{i,i+1}$ (MHz)
1→2	93,418 ± 7,010
2→3	43,962 ± 5,888
3→4	54,952 ± 6,098
4→5	38,466 ± 5,799

Table 4.13: frequency distances of the dips

For the lines you now get:

F-transition	$\Delta\nu_{meas.,FPI}$ (MHz)	$\Delta\nu_{theo.}$ (MHz)
4→3	93,418 ± 7,010	120,640
3→2	54,952 ± 6,098	63,401

Table 4.14: Comparism of experiment (with FPI) and theory

As you see the values measured using the FPI are lower than the values that are calculated with the current-wavelength function. The theoretical values are not covert by this values. The reason of the difference can be, that we're using for the frequency distance per 'mA' the full measurment and not the measurment of the single line. We're doing this, because the FPI is in the single-line measurment very noisy so its hard to count all of the peaks.

4.5 Hyperfineconstant

The Hyperfineconstant A is defined as (Köhler, 2021):

$$A = \frac{2 \cdot \Delta E_{HFS}}{F(F+1) - J(J+1) - I(I+1)} \quad (4.21)$$

Where ΔE_{HFS} is the distance between the hyperfine dips and the normal niveau.

We had not measured the normal niveau, so you can rewrite the definition of the Hyperfineconstant as the following:

$$A = \frac{2 \cdot (\Delta E_{1,2})}{F_1(F_1+1) - F_2(F_2+1)} = \frac{2h \cdot (\Delta \nu_{1,2})}{F_1(F_1+1) - F_2(F_2+1)} \quad (4.22)$$

Here is $\Delta E_{1,2}/\Delta \nu_{1,2}$ the distance between the hyperfine dip 1 and 2.

For our transitions you get:

F-transition	$A_{meas.} (10^{-26} \text{ J})$
$4 \rightarrow 3$	$1,80278 \pm 0,14997$
$3 \rightarrow 2$	$1,41395 \pm 0,19996$

Table 4.15: Hyperfineconstants for measured dips

So you get a hyperfineconstant of:

$$A_{meas.} = (1,608365 \pm 0,174965) \cdot 10^{-26} \text{ J} \quad (4.23)$$

The theoretical value is given as (Steck, 2013):

$$A_{theo.} = 1,65665 \cdot 10^{-26} \text{ J} \quad (4.24)$$

If you compare the two values, the theoretical value is in the errorrange of the measured value.

4 Data Analysis

4.6 Temperature of the probe

Through the doppler-shift the width (*full width, half maximum*) of one line gets expanded like (Wikipedia, 2021a):

$$f' = \frac{x_0}{c} \sqrt{\frac{k_B \cdot T}{m}} \quad (4.25)$$

Where f' is the shifted width, x_0 the maximum, k_B the Boltzmann-constant, m the Mass of the particle and T the Temperature.

If we want the new FWHM:

$$FWHM' = \frac{x_0}{c} \sqrt{8 \ln(2) \frac{k_B \cdot T}{m}} \quad (4.26)$$

We also know the FWHM for an gaussian-curve:

$$FWHM = \sqrt{8 \ln(2)} \cdot \sigma \quad (4.27)$$

So the Temperature for the gas is calculated as:

$$T = \frac{m}{k_B} \cdot \left(\frac{\sigma}{x_0} c \right)^2 \quad (4.28)$$

To calculate the speed of the particles, we presume it is boltzman-distributed:

$$\bar{v} = \sqrt{\frac{8k_B T}{\pi m}} \quad \hat{v} = \sqrt{\frac{2k_B T}{m}} \quad (4.29)$$

Where \bar{v} is the average and \hat{v} the most likely velocity.

So to each first dip of the absorption spectrum the gaussian-curve is fitted and the Temperature and velocitys are calculated:

T_{real} (K)	\bar{v}_{real} (m/s)	\hat{v}_{real} (m/s)	T_{calc} (K)	\bar{v}_{calc} (m/s)	\hat{v}_{calc} (m/s)
296,55	271,8	170,3	331,73	287,4	254,8
310,95	278,3	246,6	654,71	403,8	357,9
329,15	286,3	253,8	802,83	557,2	396,3

The real values (Temperature measured over the heater unit) and the calculated values differ a lot. The first value is in comparism to the others quite good, but we have no clue, why the distance between the measured and calculated temperatur is growing.

5 Summary

In summary, the results do not agree satisfactorily with the literature values. As already mentioned in the evaluation, this is mainly due to the inaccurate method of determining the wavelength and the resulting frequencies. The lines of the isotopes could not be clearly determined.

Nevertheless, it is important to follow up with the fine and hyperfine structures as well as with energy levels. With that experiment it was possible to apply our theoretical knowledge about the nuclear and atom structures.

A Protocol

Versuch Spektroskopie an Rubidium

Datum: 20.09.2021
Raum: 3.0.09 BGI

1. Versuchsaufbau

Der Versuch wird nach der Anleitung im Skript aufgebaut und justiert.

Der Versuchstisch:



Nach der Justierung wird die Intensität des Probestrahls und des Referenzstrahl in etwa gleichgesetzt, dies geschieht mithilfe des $\lambda/2$ Plättchen.

Die Intensitäten werden auf dem Messprogramm überprüft und unter „Adjust“ live beobachtet.

$\lambda/2$ – Stelle: 299°

Die Intensitätsdifferenz: >0,001

2. Messprogramm

Ai0: Quotient an D2 (Ref/Probe)

Ai1: Probestrahl

Ai2: nichts

Ai3: Referenzstrahl

Ai4: FPI an D1

x-Achse: Laderdiode current in mA

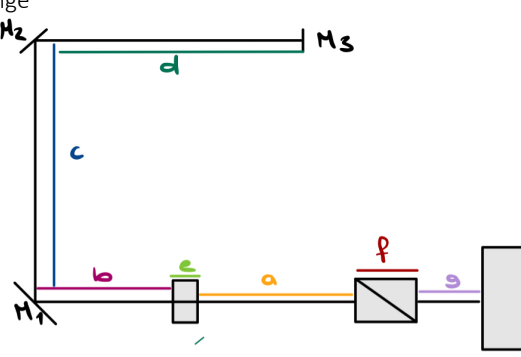
y-Achse: Amplitude in V

Dateiname: 20 09 2021_Uhrzeit_group6_name

Im Folgendem wird nur „name“ aufgeführt.

3. Messungen

Länge



$$d: (42 \pm 0,3) \text{ cm}$$

$$c: (350 \pm 0,3) \text{ cm}$$

$$b: (72,0 \pm 0,3) \text{ cm}$$

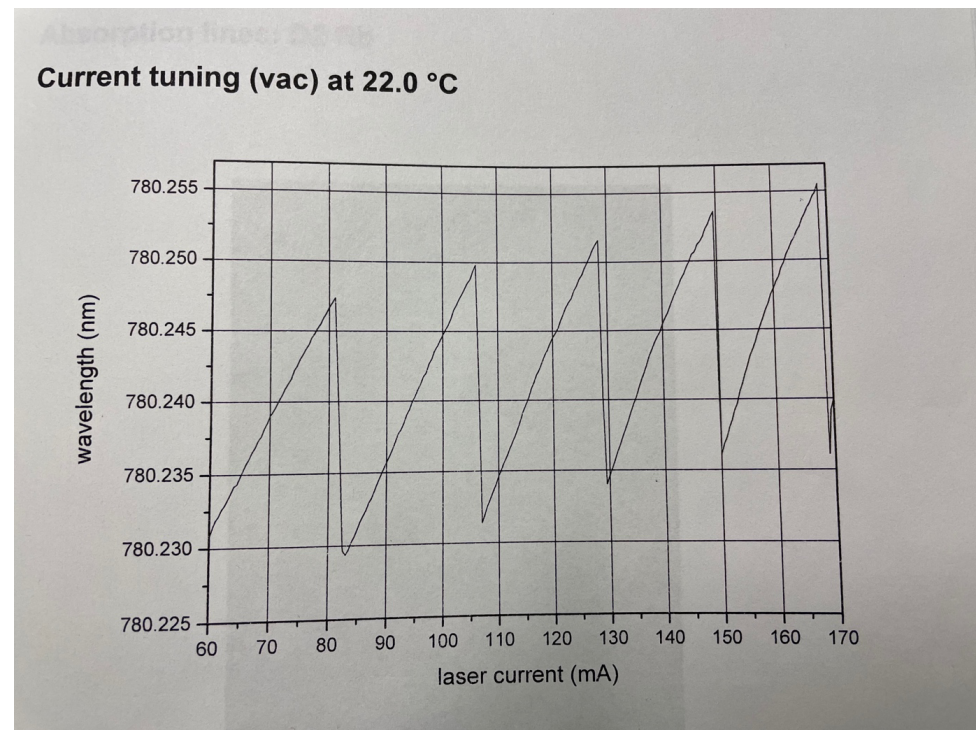
$$a: (7,9 \pm 0,3) \text{ cm}$$

$$e: (0,7 \pm 0,1) \text{ cm}$$

$$f: (1,5 \pm 0,1) \text{ cm}$$

$$g: (7,4 \pm 0,1) \text{ cm}$$

Current tuning at 22.0°



4. Daten

a. Temperatur ($23,4 \pm 0,2$)°

Messung	Current in mA	Range	Dt/pixel	Steps	Name
Alle Linien	132,0	0,4050	150	2000	23_full
Linie1	120,0	0,0200	150	2000	23_L1
Linie2	125,4	0,2000	150	2000	23_L2
Linie3	132,0	0,2000	150	2000	23_L3
Linie4	136,0	0,2000	150	2000	23_L4

b. Temperatur ($37,8 \pm 0,2$)°

Messung	Current in mA	Range	Dt/pixel	Steps	Name
Alle Linien	152,5	0,3000	150	2000	40_full
Linie1	142,3	0,0200	150	2000	40_L1
Linie2	148,2	0,0200	150	2000	40_L2
Linie3	153,8	0,0200	150	2000	40_L3
Linie4	157,0	0,0200	150	2000	40_L4

c. Temperatur ($56,0 \pm 0,2$)°

Messung	Current in mA	Range	Dt/pixel	Steps	Name
Alle Linien	154,7	0,3500	150	2000	60_full
Linie1	142,6	0,0200	150	2000	60_L1
Linie2	147,5	0,0200	150	2000	60_L2
Linie3	154,0	0,0200	150	2000	60_L3
Linie4	157,0	0,0200	150	2000	60_L4

5. Messgeräte

- **Frequenzgenerator**
RIGOL DG4062
Inventar: 97280
Channel1: 9,0 GHz, Ampl.
23.000 dBm
Channel2: deaktiviert
- **Netzteil**
RIGOL DP 831A
Inventar: 97280
- **Laser Dioden controller**
Pilot PC 500
→ Einstellung der Current in mA
Ablesefehler: 0,1 mA
- **NI-USB 6002 AD Interface**
- **Temperature Controller**
Thor Labs TC2000
Ablesefehler: 0,1°C
- **Schraubtisch**
Inventar 101273
- **Laser**
Cheetah
TEC 55
Nummer: NC-780-7016-0071
Max. Output: < 120 mW
Wellenlänge: 780nm
Max. Stoß: 140mA
- **Detektor 1**
Thor Labs
PDB2010A-M
- **Detektor 2**
Thor Labs
PDA100A-EC
- **Maßband**
Ablesefehler: 1mm
- **Interlock**
LSU-ELUB 3/170/4
→ Sicherheitsschalter Laser
- **Diverse Optische Bauelemente**

Bibliography

- KÖHLER, PROF. DR. JÜRGEN 2021 *Skript für Experimentalphysik B: Atome, Kerne und Elementarteilchen*. Vorlesungsskript, Universität Bayreuth.
- STECK, DANIEL ADAM 2013 *Rubidium 85 D Line Data*, 2.1.6.
- STECK, DANIEL ADAM 2015 *Rubidium 87 D Line Data*, 2.1.5.
- WIKIPEDIA 2021a Dopplerfreie sättigungsspektroskopie. URL https://de.wikipedia.org/wiki/Dopplerfreie_Sättigungsspektroskopie – Zugriffssdatum: 19.09.2021.
- WIKIPEDIA 2021b Lorentzkurve. URL <https://de.wikipedia.org/wiki/Lorentzkurve> – Zugriffssdatum: 25.09.2021.
- WIKIPEDIA 2021c Strahlteiler. URL <https://de.wikipedia.org/wiki/Strahlteiler> – Zugriffssdatum: 19.09.2021.
- WIKIPEDIA 2021d Verzögerungsplatte. URL <https://de.wikipedia.org/wiki/Verzögerungsplatte> – Zugriffssdatum: 19.09.2021.